A multi-step reaction scheme to simulate self-heating ignition of coal: Effects of oxygen adsorption and smouldering combustion

*Han Yuan, Franz Richter, and Guillermo Rein**

Department of Mechanical Engineering Imperial College London, London, SW7 2AZ, UK

Corresponding author email: g.rein@imperial.ac.uk

Abstract[1]

Self-heating ignition has been a fire hazard in coal production, transportation, and storage for decades. Self-heating ignition of coal is driven by two exothermic processes which are chemically and thermodynamically different: adsorption of oxygen and heterogeneous combustion (smouldering). In classical self-heating theory and previous computational studies, a lumped one-step reaction was used. However, this scheme does not differentiate the aforementioned two processes. This study develops a computational model that incorporates a 4-step reaction scheme, encompassing both adsorption and smouldering, to simulate self-heating ignition. The kinetic parameters for a bituminous coal are first obtained through inverse-modelling of thermogravimetric experimental data from the literature. Based on the 4-step reaction scheme and kinetic parameters, we simulate two sets of hot plate experiments from the literature and predict the critical ignition temperature of different sample thicknesses. These predictions are compared with the predictions using a 1-step reaction scheme. Predictions based on both schemes show a good agreement with experiments when sample thickness(L) is less than 20 mm. However, the accuracy of the model with 1-step scheme decreases as the sample thickness increases. The critical ignition temperatures predicted by the 1-step scheme become significantly higher than the 4-step scheme when L > 20 mm and at$L$= 127 mm the difference is over 12 %. According to the simulation results of the 4-step scheme, at the large-scale scenarios, adsorption is the dominant reaction before ignition and the acceleration of smouldering occurs afterwards. As 1-step reaction scheme does not differentiate adsorption and smouldering, a 4-step scheme is more suitable for realistic and large scale scenarios.

[1] Please cite this article as: H. Yuan, F. Richter and G. Rein, A multi-step reaction scheme to simulate self-heating ignition of coal: Effects of oxygen adsorption and smouldering combustion, Proceedings of the Combustion Institute, https: //doi.org/10.1016/j.proci.2020.07.016

Nomenclature

A	pre-exponential factor,1/s
c	solid specific heat capacity, J/kg-K
Cp	gas specific heat capacity, J/kg-K
D	mass diffusivity, m^2/s
E	activation energy, kJ/mol
$\bar{h}$	specific enthalpy, J/kg
h_c	convective heat transfer coefficient, W/m^2-K
h_m	diffusive mass transfer coefficient, kg/m^2-s
h_{vl}	volumetric heat loss coefficient, W/m^3-K
ΔH	change in enthalpy, MJ/kg
k	thermal conductivity, W/m-K
L	the thickness of sample, mm
$\dot{m}''$	mass flux, kg/m^2-s
M	molar mass, g/mol
n	heterogeneous reaction order
P	pressure, Pa
t	time, s
T	temperature, ^oC
x	horizontal length, mm
Y	mass fraction
z	vertical length, mm

Greeks

ε	emissivity
κ	permeability, m^2
$\bar{\rho}$	bulk density, kg/m^3
v	viscosity or stoichiometry
ϕ	porosity
$\dot{\omega}$	reaction rate, 1/s
$\dot{\omega}'''$	volumetric reaction rate, kg/m^3-s
σ	collision diameter, Å

Subscript

0	initial
a	ash
ad	adsorption
c	coal
cr	critical
f	formation
d	destruction
dr	drying
de	desorption
g	gas
hc	heterogeneous combustion
hp	hot plate
ig	ignition
j	gaseous species number
k	reaction number
N	Nitrogen
O	Oxygen
x	oxy-complexes
∞	free surface

1 Introduction

Coal has the propensity to self-heat. Self-heating is the temperature rise of a material due to exothermic processes taking place within the material bulk [1]. Self-heating can lead to ignition when the rate of heat generation is greater than the rate of heat dissipation. Self-heating ignition has been a safety concern in the production, transportation, and storage of coal for decades.

From a chemistry point of view, the self-heating ignition of coal is driven by two exothermic processes: adsorption of oxygen and heterogeneous combustion [2, 3]. Adsorption denotes the chemisorption of oxygen on the surfaces of coals with the formation of carbon-oxygen complexes, which decompose into gases at higher temperatures. Referred to as the burn-off reaction in the literature [2, 3], heterogeneous combustion (smouldering) occurs between oxygen and coal and produces ash and gases with a large amount of heat released. The two chemical pathways have been found to initiate at different temperatures: adsorption occurs first at low temperature range (usually less than 150 ^{o}C), where the increase of mass and a significant amount of heat release are observed in Thermogravimetric Analysis (TGA) and Differential Scanning Calorimetry (DSC) experiments respectively. Heterogeneous combustion accelerates and becomes the dominant reaction at high temperatures which is identified by the rapid decrease of mass in TGA curve and the heat release peak in DSC curve. This is in agreement with other findings that there is a change of dominant chemical pathway at approximately 230 ^{o}C [4] and smouldering becomes the main reaction after ignition [5]

Since adsorption initiates at a lower temperature range, it is considered to have a larger reaction rate than smouldering when the temperature is less than 150 ^{o}C [6] (the temperature condition at which coal is commonly stored and transported). In a large pile of coal, heat generated from adsorption cannot dissipate quickly and the accumulation of heat can trigger self-heating ignition. In previous computational studies [7, 8], the kinetic scheme was simplified to a lumped 1-step reaction, which does not differentiate between adsorption and smouldering. Based on the literature review, the authors hypothesized that a multi-step scheme that separates adsorption and smouldering can better

characterize the chemical processes in different temperature ranges and hence can produce more accurate simulations for the self-heating ignition of coal, especially when coal is stocked in large piles where the critical ignition temperature is low.

This study develops a computational model that incorporates a multi-step reaction scheme, including both adsorption and smouldering, to simulate the self-heating ignition of coal. We first study and inverse model the TGA experiments carried out on Pittsburgh bituminous coal [9] to obtain the kinetic parameters. The multi-step scheme and the obtained kinetic parameters are then used to simulate hot plate experiments of two different coals. The simulation results are compared blindly with experimental data and also with the predictions using a 1-step scheme to reveal the effect of multi-step kinetics.

2 4-step reaction scheme

2.1 Kinetics

The multi-step scheme used here is based on the literature [6, 10-12] and it is given by Eq.(1)~(4). Eq.(1) is the drying process. Drying affects the critical ignition temperature and ignition time [10] The mass fraction of moisture accounts for up to 33% of the total mass in fresh coals [6]. The drying of moisture content was therefore included in this scheme using the Arrhenius law, as done before in previous studies [10, 11]. With respect to the reactions of coal, as discussed in the introduction, there are two main reaction sequences during self-heating ignition: oxygen adsorption/desorption and heterogeneous combustion.

$$\mathrm{H_2O}\,(liquid) \rightarrow \mathrm{H_2O}\,(gas) \tag{1}$$

$$\mathrm{coal} + \nu_{\mathrm{ad,o}}\ \mathrm{O_2} \rightarrow \nu_{\mathrm{ad,x}}\ \mathrm{coal \cdot O_2} \tag{2}$$

$$\mathrm{coal \cdot O_2} \rightarrow gases \tag{3}$$

$$\mathrm{coal} + \nu_{\mathrm{hc,o}}\ \mathrm{O_2} \rightarrow \nu_{\mathrm{hc,a}}\ \mathrm{ash} + \nu_{\mathrm{hc,g}}\ \mathrm{gases} \tag{4}$$

During oxygen adsorption (Eq. (2)), the oxygen is adsorbed by the coal to form carbon-oxygen complexes (Coal· O_2) , which then decomposes into gases (Eq. (3)) during desorption [3, 6, 12].

Adsorption is an exothermic process, whereas subsequent desorption is endothermic. At high temperature range, heterogeneous combustion occurs between oxygen and coal, releasing large amounts of heat (Eq. (4)) [6, 12]. This multi-step effect has been identified by the significantly different behaviors at different temperature ranges observed by previous experimentalists and has been found to be generally applicable for a range of different coal types, including Bituminous coal [13], Subbituminous coal [14], and Lignite Coal [6].

All the reactions depend on temperature [12] as well as on the mass fractions of the condensed-phase reactants (Y_i, i can be water/coal/coal$\cdot O_2$) and oxygen (Y_O) [3, 15]. Their reaction rates follow the Arrhenius law [12]. The rate for reaction k is expressed using Eq. (5), where $n_{k,i}$ and $n_{k,O}$ represent the reaction order of the condensed-phase reactants and oxygen respectively.

$$\dot{\omega}_k = A_k e^{-E/RT} Y_i^{n_{k,i}} Y_O^{n_{k,O}} \tag{5}$$

2.2 Inverse modelling of microscale experiments

The aim of our study was to use a multi-step scheme that differentiates adsorption and heterogeneous combustion to simulate self-heating ignition. Therefore, we first analyzed the kinetics by studying TGA experiments and obtained the corresponding kinetic parameters through inverse modelling [16]. The TGA experiments of Pittsburgh bituminous coal [9] were chosen as it was the only type of coal that the authors could find in the literature with enough high-fidelity data for both TGA experiments (with data at different heating rates) and self-heating experiments. The inverse modelling was conducted using the evolutionary algorithm AMALGAM [17]. AMALGAM has been used to study the kinetics of different materials [16] and is particularly suitable for the inverse modelling of multi-step reaction schemes [18]. Eq.(6) presents the objective function for optimization, the same as that used in [16]

$$\phi = \sum_j \left(\frac{1}{N_1} \sum_{N_1} \left(\frac{m_e - m_p}{\delta_{m_e}} \right)^2 + \frac{1}{N_2} \sum_{N_2} \left(\frac{\dot{m}_e - \dot{m}_p}{\delta_{\dot{m}_e}} \right)^2 \right) \quad (6)$$

Where ϕ is the error to be minimized during optimization, j refers to different heating rates, N the number of data points, m the sample mass, $\dot{m}$ the mass loss rate, and σ the uncertainty. The subscripts e and p refer to data from experiments and predictions. The number of points (N) was determined by the experimental points available. The implementation of the TGA model and the algorithm has been presented in detail in [16]. Table 1 lists the resulting optimised kinetic parameters obtained from inverse modelling and their corresponding value ranges set for optimization were obtained from literature. The values of $\nu_{ad,x}$ and $\nu_{hc,g}$ were not optimized directly but set through mass conservation in the corresponding reactions (i.e $\nu_{ad,x}$= 1+ $\nu_{ad,o}$ in Eq.(2).;$\nu_{hc,g}$ = 1+ $\nu_{hc,O}$ - $\nu_{hc,a}$ in Eq.(4))

Table 1. The kinetic parameters for the 4-step reaction scheme obtained via inverse modelling

Parameter	Optimized value	Range for search	Ref.
$\lg A_{dr}$ (log s^{-1})	8.6	[6.0, 8.7]	[11]
E_{dr} (kJ/mol)	65.6	[54.8, 71.3]	[11]
$n_{dr,w}$ (-)	2.7	[1.7, 2.8]	[11]
$\lg A_{ad}$ (log s^{-1})	1.52	[1.0,8.4]	[14]
E_{ad} (kJ/mol)	58.8	[7.9,83.0]	[3, 19]
$n_{ad,c}$ (-)	1.98	[0,2]	[20]
$n_{ad,o}$ (-)	1.50	[0,2]	[20]
$\nu_{ad,o}$ (kg/kg)	0.11	[0,2]	[15]
$\nu_{ad,x}$(kg/kg)*	1.11	N/A	N/A
$\lg A_{de}$ (log s^{-1})	1.98	[5.0, 10.3]	[14]
E_{de} (kJ/mol)	104.2	[65,150]	[3, 14, 19]
$n_{de,x}$(-)	0.27	[0,2]	N/A
$\lg A_{hc}$ (log s^{-1})	4.55	[1.0, 9.3]	[12]
E_{hc} (kJ/mol)	95.5	[43.4,105.0]	[14, 15]
$n_{hc,c}$ (-)	0.98	[1.2,2.1]	[21]
$n_{hc,o}$ (-)	0.93	[0.2,1.0]	[20]
$\nu_{hc,o}$(kg/kg)	2	[0,2]	[7, 9]
$\nu_{hc,a}$ (kg/kg)	0.12	[0,0.2]	[9]
$\nu_{hc,a}$(kg/kg)*	3.12	N/A	N/A

*denotes the values not optimized but set via mass conservation

Figure 1 compares the simulations using inverse-modelled kinetics parameters and TGA experimental data in [9]. From 30 to 200 ^{o}C, the sample mass gradually decreased by 4% due to drying.

From 200 to 350 °C, the sample mass remained approximately the same, with less than a 1% increase induced by the adsorption of oxygen. After 350 °C, the sample mass decreased rapidly, indicating the acceleration of combustion. The simulations agree well with experiments with the maximum error less than 3%.

Figure 2 compares the rates of different reactions at different temperatures using the prediction at the heating rate of 5 °C/min. Drying is the main reaction that occurs below 200 °C. Above 200 °C, adsorption and smouldering increase significantly, followed by the acceleration of desorption at 300 °C. Smouldering is the dominant reaction after 400 °C and its reaction peak is 4 times higher than adsorption. However, a detailed examination of the reactions occurring between 80 and 180 °C (the zoom-in view) reveals that adsorption is triggered first at around 100°C whereas smouldering is negligible. Even though the reaction rate of adsorption is small as observed in this microscale experiment, it can be essential when coal is stocked in large piles. At large scales, heat dissipation is extremely slow inside coal piles, and small amounts of heat can accumulate continuously and eventually lead to self-heating ignition in the long term. We will examine this mechanism in detail in the following section.

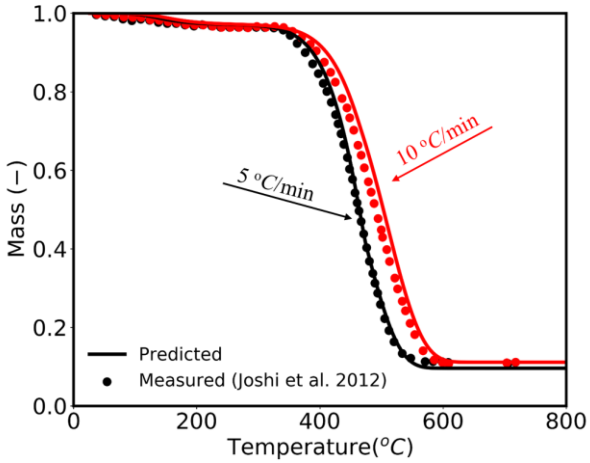

Figure 1 Comparison of simulation and experimental data for the TGA experiments in [9]

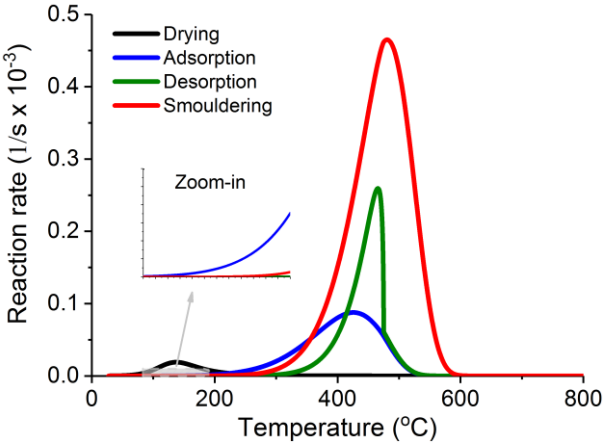

Figure 2 Predicted reaction rates as a function of temperature at the heating rate of 5°C/min

3 Simulation of self-heating experiment

The simulations in this section are for two hot plate experiments. The first was conducted by Park, Rangwala *et al.* [22] who used the same coal as used in the aforementioned TGA experiments [9]. To conduct blind predictions of the present model, the second was another set of hot plate experiments [23] using a different coal (South Africa coal). Figure 3 shows the schematic of an experimental set up, where the thickness of the layer is 12.7mm is given as an example. The hot plate experiment aims to measure the critical hot plate temperature (T_{ig}) that triggers the ignition of a dust layer. Different thicknesses (L ranges from 5 to 30 mm) were studied in the two set of experiments. Several thermocouples were mounted evenly at the centreline of the sample to monitor the temperature changes. The ignition was considered to occur when the temperature measurement at any thermocouple was 50 °C higher than the hot plate [24].

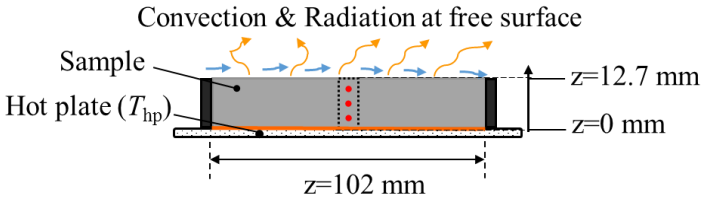

Figure 3 Schematic of hot plate experiment [22] for layer thickness L = 12.7 mm; The positions of the three thermocouples are z=4 mm , 7 mm, and 10 mm as marked by the red dots

3.1 Governing equations

The computational model is built based on an open source code- Gpyro [7, 25].The governing equations are Eqs.(7)-(12), which impose the conservations of (7) mass, (8) species and (9) energy in the condensed phase, as well as (10) mass, (11) species, and (12) momentum (Darcy's law) in the gas phase. Subscripts i and j refer to the condensed-phase species and gas species respectively. All the other symbols are explained in the nomenclature table. Further details on the formulation of Gpyro and solution method can be found in [25].

$$\frac{\partial \bar{\rho}}{\partial t} = -\dot{\omega}'''_{fg} \tag{7}$$

$$\frac{\partial \left(\bar{\rho} Y_i\right)}{\partial t} = \dot{\omega}'''_{fi} - \dot{\omega}'''_{di} \tag{8}$$

$$\frac{\partial \left(\bar{\rho}\bar{h}\right)}{\partial t} = k\frac{\partial}{\partial z}\left(\frac{\partial T}{\partial z}\right) + \dot{\omega}'''_{di}(-\Delta H_i) - h_{vl}(T - T_\infty) \tag{9}$$

$$\frac{\partial}{\partial t}(\rho_g \bar{\phi}) + \frac{\partial \dot{m}''}{\partial z} = \dot{\omega}'''_{fg} \tag{10}$$

$$\frac{\partial}{\partial t}(\rho_g \bar{\phi} Y_j) + \frac{\partial}{\partial z}(\dot{m}'' Y_j) = -\frac{\partial}{\partial z}(\bar{\phi}\rho_g D\frac{\partial Y_j}{\partial z}) + \dot{\omega}'''_{fj} - \dot{\omega}'''_{dj} \tag{11}$$

$$\dot{m}'' = -\frac{\bar{\kappa}}{\nu}\left(\frac{\partial p}{\partial z} - g\rho_g\right) \qquad \left(\rho_g = \frac{P\overline{M}}{RT}\right) \tag{12}$$

In the model, the averaged properties in each cell were calculated by weighting appropriate mass or volume fractions. All gaseous species were set to have unit Schmidt numbers, and equal diffusion coefficient and specific heat. The thermal properties of all species were assumed to be independent of temperature.

In the hot plate experiment since the thickness of the layer is significantly smaller than its horizontal dimension, the lateral heat and mass transfer can be neglected [7]. We therefore used a 1D model to simulate this experiment. The boundary conditions were the same as presented in our previous study [7]: Convection and reradiation are considered on the top free surface. Fixed temperature and impermeable boundary conditions are applied to the bottom. At t = 0, the mass fraction for moisture and coal is Y_w=0.04 and Y_c = 0.96 respectively. The initial temperature for both coal and

air inside the sample is the same as the ambient temperature (T_∞= 20°C).

3.2 Parametrization

The kinetic parameters obtained through inverse modelling (Table 1) were used for the simulations of hot plate experiments. It is shown in previous studies [6, 26] that to accurately measure the reaction rate of adsorption in TGA experiments low heating rates (usually less than 5 °C/min) are more desirable. This is because the adsorption rate tends to be underestimated at high heating rates. The TGA experiments used for the optimization are at heating rates of 5 °C/min and 10 °C/min. As a result, the lgA_{ad} (pre-exponential factor) and E_{ad} (activation energy) for adsorption were set to 2.0 log s^{-1} and 56 kJ/mol here to offset the underestimation of the adsorption rate. The experiments used for inverse-modelling were conducted using bituminous Pittsburgh coal. The performance of the model was evaluated by blindly simulating (namely using the same kinetic parameters as used for Pittsburgh coal) the self-heating experiments in [23], which also used bituminous coal, the same type coal as Pittsburgh coal.

The values for the heat of reaction were also obtained from the literature. The drying process is endothermic and the heat of reaction is 2.26MJ/(kg H_2O) [11]. Heat of adsorption is reported to range from 4 to 14 MJ/(kg coal) [13] for bituminous coal and a middle-range value of 10 MJ/(kg coal) is used here. The subsequent desorption is endothermic and requires around a quarter of the heat released during adsorption according to the DSC experiments in [27]. The heat of desorption is set to be 2.5 MJ/(kg coal) accordingly. For heterogeneous combustion, the heat of reaction for Pittsburgh bituminous coal(PS) is 29.8 MJ/(kg coal) [22] and the heat of reaction for South Africa bituminous coal(SA) is 27.4 MJ/(kg coal) [23]

Table 2 lists the thermal-physical parameters for solid species. For the Pittsburgh coal and South Africa coal, their densities (ρ), heat conductivities (k), and porosities (ϕ) were reported in [22] and

[23] respectively. Their heat capacity c and permeability κ are obtained from [28] and [29] respectively. $\mathrm{Coal \cdot O_2}$ is assumed to have the same properties as coal, except for density, which increases by 11% due to the oxygen adsorption (as shown by the $v_{ad,o}$ (kg/kg) in Table 1). For ash, the density and permeability are obtained from [30] and [31] respectively. The other properties of ash are from [32].

Table 2. The values of thermal-physical parameters for solid species used in the simulations

	Unit	Coal (PS)	$\mathrm{Coal \cdot O_2}$ (PS)	Ref.	Coal (SA)	$\mathrm{Coal \cdot O_2}$ (SA)	Ref.	Ash	Ref.
ρ	kg m^{-3}	532	590	[22]	600	660	[23]	800	[30]
k	W m^{-1}K^{-1}	0.1	0.1	[22]	0.1	0.1	[23]	0.06	[32]
c_p	J kg^{-1} K^{-1}	1080	1080	[28]	1080	1080	[28]	880	[32]
ϕ	-	0.59	0.65	[22]	0.50	0.58	[23]	0.03	[32]
κ	m^2	$5\cdot10^{-14}$	$5\cdot10^{-14}$	[29]	$5\cdot10^{-14}$	$5\cdot10^{-14}$	[29]	10^{-16}	[31]

3.3 Simulation results

The simulation starts from the case L = 12.7mm in [22] as this case has a lower measurement uncertainty than other three cases as presented in [22]. It is seen in Figure 4, the predicted temperature histories predicted are compared with experimental data [22] and previous simulations using the 1-step reaction [7]. Both reaction schemes successfully predict the occurrence of self-heating ignition at T_{hp}= 215 ^{o}C and capture the significant increase of temperature after 3000s. Comparatively, the 4-step model shows a slightly better agreement with experimental data at beginning (where temperatures are below 200 ^{o}C) and end (smouldering stage): Before t = 1250 s, the temperatures predicted by the 4-step scheme is around 15 ^{o}C lower than 1-step scheme due to the endothermic drying; After t = 3000 s, the 4-step model better predicts the temperature increase at z=4 mm, which is underestimated by around 40 ^{o}C in the 1-step model. This improvement is because the differentiation of smouldering and adsorption in the 4-step scheme can lead to a better kinetic description of the whole process and hence a more accurate prediction.

Figure 5(a) compares the predicted T_{ig}s via two different reaction schemes with experimental measurements in [22]. Both 4-step and 1-step schemes give satisfactory predictions of T_{ig} for the 4

experiments. The predicative error is less than 5^{o}C and is within the measurement uncertainty. Based on the model, we further simulated an additional set of hot plate experiments which use South African bituminous coal [23] and compared the simulations results with experimental data as shown in Figure 5(b). It is seen that even though at L = 10 mm and 20 mm the predictions of these two schemes are equally satisfactory, the predictive error of the 1-step reaction becomes significant at L= 30 mm. At this thickness, the 1-step scheme over-predicts the T_{ig} by 4 ^{o}C, (which is larger than the measurement uncertainty), whereas the error of 4-step reaction scheme is only 1 ^{o}C. Since the kinetic parameters used in the simulations are the same as that in Figure 5(a) (See the explanation in Section 3.2), this can be regarded as a blind validation of 4-step scheme model. The predicting difference between two schemes grows with sample thickness. At L = 127 mm, the difference is larger than 15 ^{o}C (12%). Based on the simulations, the authors conclude that the 1-step reaction model will over-predict the T_{ig} as L increases. This finding is supported by the research conducted by Reddy, Amyotte *et al.* [33], who also used a 1-step reaction scheme to simulate hot plate experiments. In their study, when L increased to 50 mm the 1-step model overpredicted the experimental data by 20^{o}C.

The authors think that the over-prediction is because 1-step scheme does not differentiate the two exothermic reactions that occur at different temperature ranges. In the small-scale scenario, where the critical temperature is high and the self-heating ignition is mainly influenced by smouldering, the one-step reaction scheme might still be applicable. However, as the sample thickness increases, the critical temperature decreases. The effect of adsorption becomes essential and therefore needs to be considered separately using a multi-step scheme.

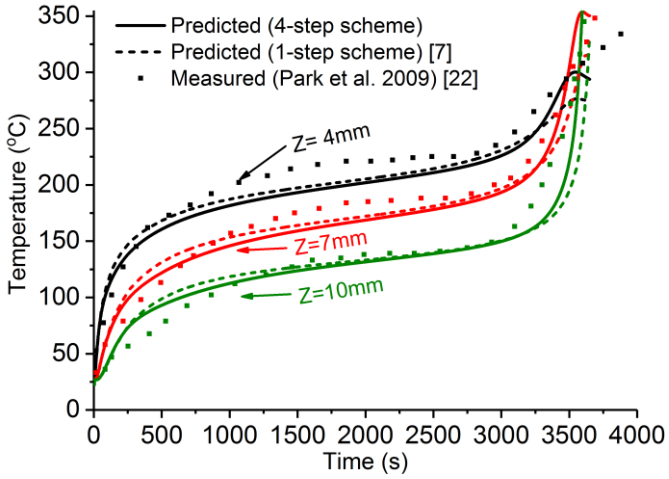

Figure 4 Comparison of predicted and measured [22] temperature histories for case L = 12.7 mm at supercritical condition (T_{hp}= 215 °C)

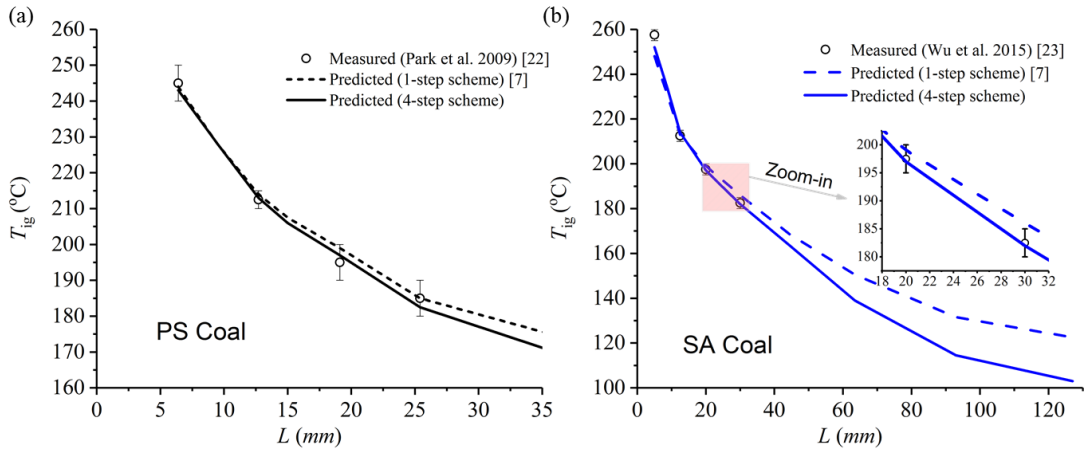

Figure 5 Comparison of predicted and measured T_{ig} [22, 23] for the hot plate experiment ; (a) is for PS Coal in [22] (b) is for SA Coal in [23];Symbols represent experimental data; solid and dash lines represent predictions of 4-step and 1-step reaction scheme respectively

The effect of different reactions at different thickness is further analyzed in Figure 6 and Figure 7. Figure 6 shows the predicted transient profiles of temperature and reaction rates for the supercritical condition (T_{hp} = 215 °C) at L=12.7 mm. In this case, smouldering is the main reaction even before ignition: at t= 3000s smouldering reaction rate is already two times larger than the adsorption rate. In other words, self-heating ignition is driven by adsorption and smouldering but mainly triggered by smouldering. After t = 3400s, coal has ignited and the temperature increases rapidly, leading to the spread of smouldering.

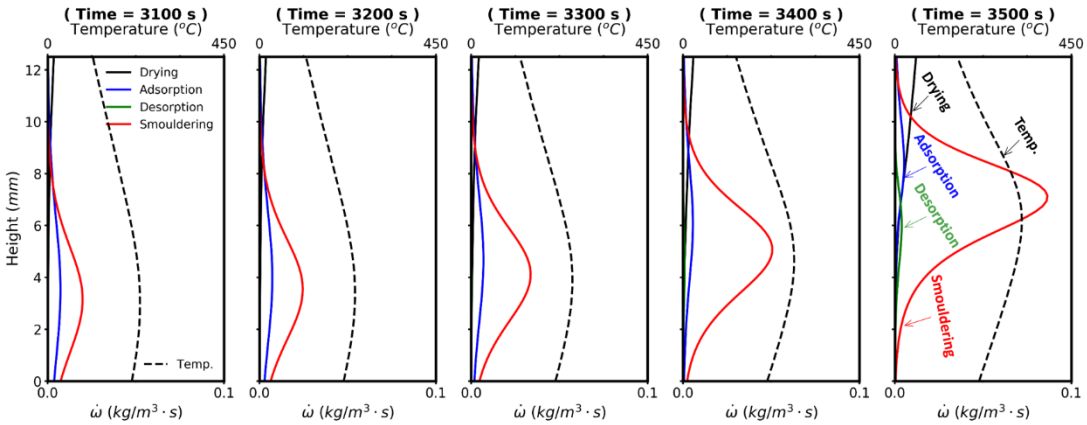

Figure 6 Predicted profiles of temperature (dash line) and reaction rate (solid line) at different time steps for the case L = 12.7 mm at T_{hp} = 215 °C

However, adsorption becomes essential at a larger thickness (L = 127 mm) as shown in Figure 7. Under a lower hot plate temperature (T_{hp} = 103 °C), adsorption is the dominant reaction before ignition and at t = 51h the adsorption rate is 10 times larger than smouldering. At that time, the heat release during adsorption accumulates in the sample and the temperature keeps increasing from 51 h to 63 h. At t= 63 h, smouldering reaction starts to spread with significant temperature rises. There is an evident transition of chemical pathway from adsorption to smouldering before and after ignition. According to these results, at large-scale scenarios self-heating ignition of coal is mainly trigger by adsorption and then smouldering takes over after ignition. This hypothesis agrees with previous findings that adsorption serves as a ladder reaction to more energetic and faster heterogeneous combustion [12].

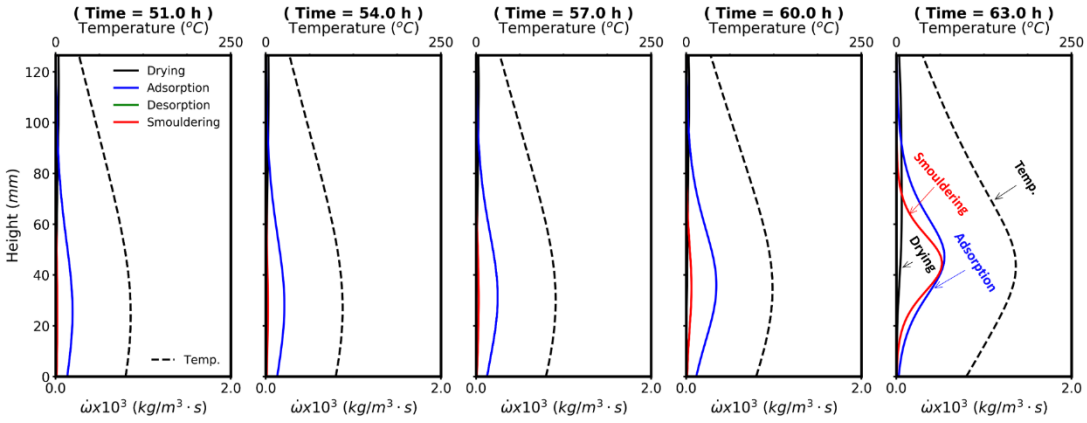

(a)

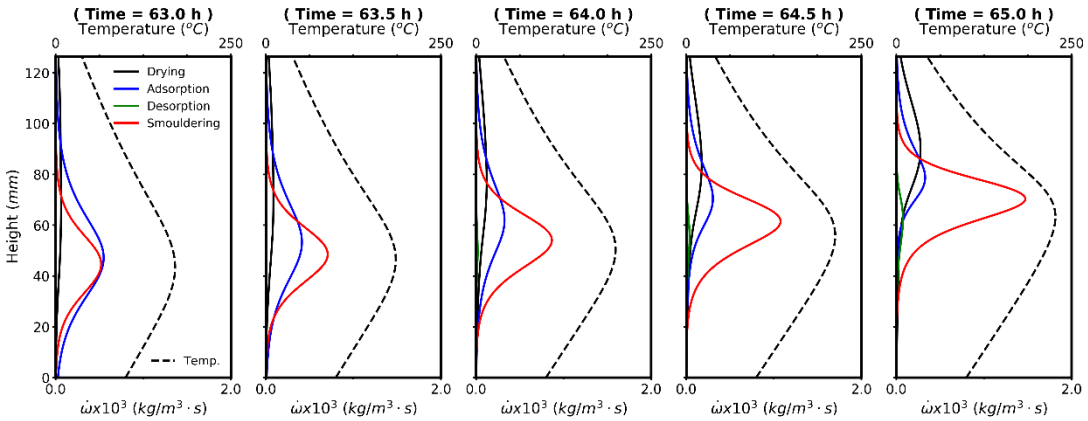

(b)

Figure 7 Predicted profiles of temperature (dash line) and reaction rate (solid line) at different time steps for the case L = 127 mm at T_{hp} = 103 °C

4 Conclusions

This study develops a computational model that incorporates a 4-step reaction scheme, including drying, adsorption, desorption, and smouldering to simulate the self-heating ignition of coal. According to the inverse-modelling results of microscale experiments, adsorption initiates at a lower temperature than smouldering, which agrees with previous findings in the literature. Based on the kinetic parameters obtained from inverse modelling, we simulate two sets of hot plate experiments and compare the simulations with the 1-step scheme model in [7]. Both 4-step and 1-step schemes can accurately predict the T_{ig} for thin layers. However, as the sample thickness increases, the T_{ig} predicted by 1-step scheme becomes significantly higher than that by the 4-step scheme and the difference is larger than 12 % at L= 127 mm. Further comparing the reaction rates of different reactions, we find that at the large-scale scenarios, adsorption is the dominant reaction before ignition and the acceleration of smouldering occurs afterwards. These findings lead us to hypothesize that in the large-scale scenario self-heating ignition is essential. As 1-step reaction scheme does not differentiate adsorption and smouldering, a 4-step scheme is more suitable for large scale scenarios, such as coal piles. In summary, this study deepens our understanding of adsorption and smouldering during self-heating ignition and presents a model that can simulate this phenomenon more accurately.

Acknowledgments

This research was funded by European Research Council (ERC) Consolidator Grant HAZE (682587), EPSRC (G01734) and the President's PhD Scholarship Scheme of Imperial College London.

References

[1] D.A. Frank-Kamenetskii, Diffusion and heat transfer in chemical kinetics, Plenum Press, New York, 1969.
[2] S. Krishnaswamy, S. Bhat, R.D. Gunn, P.K. Agarwal, Low-temperature oxidation of coal. 1. A single-particle reaction-diffusion model, *Fuel* 75:333-343 (1996).
[3] H. Wang, B. Dlugogorski, E. Kennedy, Kinetic modeling of low-temperature oxidation of coal, *Combust. Flame* 131:452-464 (2002).
[4] A. Kam, A. Hixson, D. Perlmutter, The oxidation of bituminous COAL—II experimental kinetics and interpretation, *Chem. Eng. Sci.* 31:821-834 (1976).
[5] V.N. Marinov, Self-ignition and mechanisms of interaction of coal with oxygen at low temperatures. 2. Changes in weight and thermal effects on gradual heating of coal in air in the range 20–300 C, *Fuel* 56:158-164 (1977).
[6] C. Avila, T. Wu, E. Lester, Estimating the Spontaneous Combustion Potential of Coals Using Thermogravimetric Analysis, *Energy Fuels* 28:1765-1773 (2014).
[7] H. Yuan, F. Restuccia, F. Richter, G. Rein, A computational model to simulate self-heating ignition across scales, configurations, and coal origins, *Fuel* 236:1100-1109 (2019).
[8] A.K. Sahu, K.A. Joshi, V. Raghavan, A.S. Rangwala, Comprehensive numerical modeling of ignition of coal dust layers in different configurations, *Proc. Combust. Inst.* 35:2355-2362 (2015).
[9] K. Joshi, V. Raghavan, A.S. Rangwala, Effect of Weathering of Coal and Organic Dusts on Their Spontaneous Ignition, *Fire Technol.* 49:843-856 (2012).
[10] C. Lohrer, M. Schmidt, U. Krause, A study on the influence of liquid water and water vapour on the self-ignition of lignite coal-experiments and numerical simulations, *J. Loss. Prevent. Proc. Ind.* 18:167-177 (2005).
[11] X. Huang, G. Rein, Smouldering combustion of peat in wildfires: Inverse modelling of the drying and the thermal and oxidative decomposition kinetics, *Combust. Flame* 161:1633-1644 (2014).
[12] B. Li, G. Chen, H. Zhang, C. Sheng, Development of non-isothermal TGA–DSC for kinetics analysis of low temperature coal oxidation prior to ignition, *Fuel* 118:385-391 (2014).
[13] O. Senneca, P. Salatino, L. Cortese, Assessment of the thermochemistry of oxygen chemisorption and surface oxide desorption during looping combustion of coal char, *Proc. Combust. Inst.* 34:2787-2793 (2013).
[14] S. Krishnaswamy, R.D. Gunn, P.K. Agarwal, Low-temperature oxidation of coal. 2. An experimental and modelling investigation using a fixed-bed isothermal flow reactor, *Fuel* 75:344-352 (1996).
[15] G.G. Karsner, D.D. Perlmutter, Model for coal oxidation kinetics. 1. Reaction under chemical control, *Fuel* 61:29-34 (1982).
[16] F. Richter, G. Rein, Pyrolysis kinetics and multi-objective inverse modelling of cellulose at the microscale, *Fire Safety J.* 91:191-199 (2017).
[17] J.A. Vrugt, B.A. Robinson, Improved evolutionary optimization from genetically adaptive multimethod search, *Proceedings of the National Academy of Sciences* 104:708-711 (2007).
[18] D.M.J. Purnomo, F. Richter, M. Bonner, R. Vaidyanathan, G. Rein, Role of optimisation method on kinetic inverse modelling of biomass pyrolysis at the microscale, *Fuel* 262:(2020).
[19] N.M. Laurendeau, Heterogeneous kinetics of coal char gasification and combustion, *Prog. Energy Combust. Sci.* 4:221-270 (1978).

[20] E.M. Suuberg, M. Wójtowicz, J.M. Calo, Reaction order for low temperature oxidation of carbons, *Symposium (International) on Combustion* 22:79-87 (1989).
[21] Z. Song, H. Fan, J. Jiang, C. Li, Insight into effects of pore diffusion on smoldering kinetics of coal using a 4-step chemical reaction model, *J. Loss. Prevent. Proc. Ind.* 48:312-319 (2017).
[22] H. Park, A.S. Rangwala, N.A. Dembsey, A means to estimate thermal and kinetic parameters of coal dust layer from hot surface ignition tests, *J. Hazard. Mater.* 168:145-155 (2009).
[23] D. Wu, X. Huang, F. Norman, F. Verplaetsen, J. Berghmans, E. Van den Bulck, Experimental investigation on the self-ignition behaviour of coal dust accumulations in oxy-fuel combustion system, *Fuel* 160:245-254 (2015).
[24] ASTM-E2021, Standard test method for hot-surface ignition of dust layers, *ASTM International*:(2015).
[25] C. Lautenberger, C. Fernandez-Pello, Generalized pyrolysis model for combustible solids, *Fire Safety J.* 44:819-839 (2009).
[26] Y. Zhang, J. Wang, S. Xue, Y. Wu, Z. Li, L. Chang, Evaluation of the susceptibility of coal to spontaneous combustion by a TG profile subtraction method, *Korean J. Chem. Eng.* 33:862-872 (2016).
[27] D.K. Seo, S.S. Park, Y.T. Kim, J. Hwang, T.-U. Yu, Study of coal pyrolysis by thermo-gravimetric analysis (TGA) and concentration measurements of the evolved species, *J. Anal. Appl. Pyrolysis* 92:209-216 (2011).
[28] J.E. Callanan, K.M. McDermott, *Specific heat measurements of two premium coals* Report No.CONF-870802, National Bureau of Standards, 1984.
[29] Z. Pan, L.D. Connell, Modelling permeability for coal reservoirs: a review of analytical models and testing data, *International Journal of Coal Geology* 92:1-44 (2012).
[30] R. Webb, J. Stormont, M. Stone, B. Thomson, Characterizing the unsaturated and saturated hydraulic properties of coal combustion by-products in landfills of Northwestern New Mexico, *J. Am. Soc. Min. Recla* 3:70-99 (2014).
[31] T. Sinsiri, P. Chindaprasirt, C. Jaturapitakkul, Influence of fly ash fineness and shape on the porosity and permeability of blended cement pastes, *International Journal of Minerals, Metallurgy, and Materials* 17:683-690 (2010).
[32] X. Huang, G. Rein, Upward-and-downward spread of smoldering peat fire, *Proc. Combust. Inst.* 37:4025-4033 (2019).
[33] P.D. Reddy, P.R. Amyotte, M.J. Pegg, Effect of inerts on layer ignition temperatures of coal dust, *Combust. Flame* 114:41-53 (1998).